
Semantics-Preserving Evasion of LLM Vulnerability Detectors

Luze Sun^{1,2} Alina Oprea¹ Eric Wong²

Abstract

LLM-based vulnerability detectors are increasingly deployed in security-critical code review, yet their resilience to evasion under behavior-preserving edits remains poorly understood. We evaluate detection-time integrity under a semantics-preserving threat model by instantiating diverse behavior-preserving code transformations on a unified C/C++ benchmark ($N=5000$), and introduce a metric of joint robustness across different attack methods/carriers. Across models, we observe a systemic failure of semantic invariant adversarial transformations: even state-of-the-art vulnerability detectors perform well on clean inputs while predictions flip under behavior-equivalent edits. Universal adversarial strings optimized on a single surrogate model remain effective when transferred to black-box APIs, and gradient access can further amplify evasion success. These results show that even high-performing detectors are vulnerable to low-cost, semantics-preserving evasion. Our carrier-based metrics provide practical diagnostics for evaluating LLM-based code detectors.

1. Introduction

Software vulnerabilities remain among the most exploited attack vectors, driving rapid adoption of automated detection in modern continuous integration pipelines (Verizon, 2025; Microsoft, 2025). LLM-based detectors are now integrated into code review workflows at scale. This raises a security-critical question: **do such detectors satisfy semantic invariance**, or specifically, can an attacker evade detection using perturbations where **the transformed program remains strictly compilable and retains the underlying vulnerability**? If the latter holds, vulnerable code could reliably slip through automated security checks via innocuous transformations, including renaming identifiers,

¹Northeastern University ²University of Pennsylvania. Correspondence to: Luze Sun <sun.luz@northeastern.edu>.

inserting comments, injecting dead-branch code, or adding preprocessor-guarded code, while leaving the underlying exploit fully intact. Existing research has highlighted the broad spectrum of adversarial vulnerabilities in LLMs (Fu et al., 2024; Vassilev et al., 2025). Prior adversarial methods often ignore syntactic constraints, producing perturbations that break compilation or alter program logic (Ebrahimi et al., 2018). These invalid edits are practically useless: they cannot preserve the vulnerability’s executable behavior. As illustrated in Figure 1, effective evasion presents a dual challenge: naive GCG attack (Middle) breaks compilation, while randomized semantic edits (Right) often fail to evade detection. A valid attack must simultaneously satisfy the compiler’s strict syntax rules and the adversary’s evasion objective (Left).

More general-purpose LLM safety evaluations, on the other hand, primarily prioritize preventing harmful *outputs*, such as toxic content and jailbreak-style policy violations (Derczynski et al., 2024; Wei et al., 2025). Vulnerability detection, however, confronts an orthogonal integrity threat: adversaries need not induce malicious generation; they only need to make the detector *oblivious* to an existing vulnerability through behavior-preserving edits. This exposes a gap in current evaluation practices: standard safety probes emphasize output harmfulness, while clean-accuracy benchmarks ignore robustness under semantic-preserving transformations. Consequently, a detector can appear safe under toxicity-focused evaluations and achieve strong benchmark scores, yet remain brittle to innocuous perturbations in real-world deployment.

To bridge this gap, we present a systematic evaluation framework for detection-time integrity under a semantics-preserving threat model. We instantiate multiple behavior-equivalent attack surfaces and evaluate both open-weight and proprietary models (via surrogate transfer) on a unified C/C++ benchmark. Beyond per-attack evasion, we introduce *complete resistance*, measuring the fraction of vulnerabilities that withstand all semantics-preserving transformations. We make the following contributions:

1. **First Gradient-Based Evaluation of Semantic Invariance under Carrier Constraints.** We combine gradient-driven optimization with carrier-constrained perturbations to expose LLM detector vulnerabilities. Preprocessor-style carriers (`#ifdef`, `macros`) achieve

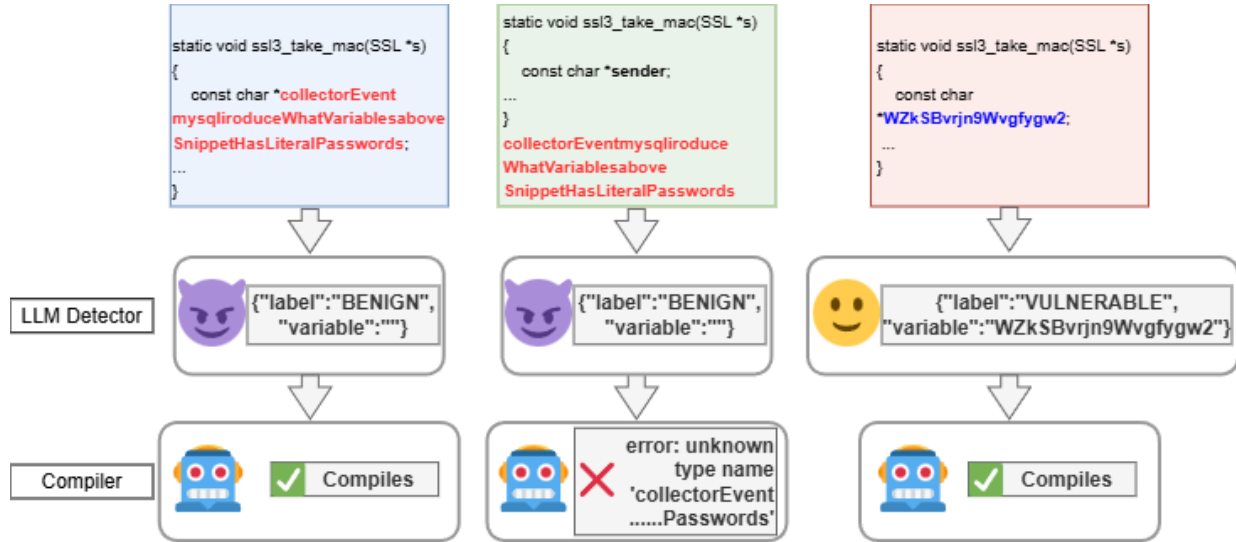


Figure 1. **Why carrier-constrained optimization matters.** **Left:** Carrier-constrained GCG via identifier substitution preserves compilation and flips the detector to BENIGN. **Middle:** Naively appending a GCG-optimized string breaks compilation, so it is not a valid semantics-preserving evasion. **Right:** Unoptimized semantics-preserving edits remain compilable but typically fail to evade detection. Red denotes the GCG-optimized identifier, blue denotes a random identifier, and boldface highlights the original identifier.

high success rates via universal triggers, contrasting with search-based methods (Jiang et al., 2026). We introduce Complete Resistance (CR) to measure joint robustness across carriers.

- Exposing the Fragility of High-Performing Detectors.** We show that models achieving 70%+ clean accuracy collapse under minimal perturbations: fewer than 13% of vulnerabilities resist all carrier types (CR < 13%), meaning 87% of “detected” threats can be evaded by at least one semantics-preserving edit (e.g., `#ifdef` insertion). High benchmark performance masks critical robustness failures. Detectors succeed on benign inputs but fail severely when code undergoes innocuous transformations.
- High Exploitability of Black-box APIs via Low-barrier Transfer.** We reveal that universal adversarial strings optimized on small surrogate models transfer effectively to closed-source models like GPT-4o without additional optimization.

2. Related Work

Datasets for Vulnerability Detection. Benchmarks for evaluating vulnerability detectors consist of labeled C/C++ functions sourced from real-world projects. Early datasets like BigVul and DiverseVul contain label noise and train-test leakage (Chen et al., 2023; Fan et al., 2020), while PrimeVul addresses these issues through manual curation and stricter deduplication (Ding et al., 2024). Since our adversarial evaluation requires clean labels—a mislabeled “vulnerable” sample would falsely appear robust—we adopt PrimeVul’s protocols and extend them with carrier-specific

controls (§4.1).

LLMs for Vulnerability Detection. Recent benchmarks, such as (Khare et al., 2025), report that state-of-the-art LLMs can achieve promising performance on standard datasets. However, other studies indicate that code language models remain unreliable for *detection* in realistic settings, paralleling similar fragility observed in code reasoning tasks (Orvalho & Kwiatkowska, 2025), highlighting the need to evaluate robustness beyond clean accuracy (Ding et al., 2024). While separate efforts benchmark the *security of generated code* (e.g., SafeGen-style evaluations), our focus is strictly on *detection-time* robustness under semantics-preserving edits, not on generation safety (Li et al., 2025).

Concurrently, recent work studies input-side defenses for adversarial transformations on code LMs. Evaluate-and-Purify proposes EP-Shield, using an LLM-as-a-judge to assess naturalness and purify identifier-substitution adversarial examples to restore predictions (Mu et al., 2025).

Our work is complementary: we focus on attack-centric robustness evaluation under a semantics-preserving threat model spanning identifier substitution, comment-carrier insertion, preprocessor-based insertions, and dead-branch code carrier, and report metrics (ASR, Complete Resistance, Transferability) that can also be used to quantify the gains of such purification wrappers across attack surfaces.

Code-Specific Adversarial Attacks on Vulnerability Detection. Adversarial attacks on code models span multiple representations. NatGVD (Rath et al., 2025) modifies graph structures for GNN detectors, while neural binary analyzers face syntactic mutation risks (Bundt et al., 2023). We

introduce gradient-driven, carrier-constrained analysis to address this gap. Our universal triggers reveal that preprocessor carriers achieve 18%–99% ASR variance across models, fundamentally differing from identifier-based attacks. We propose Complete Resistance (CR) to measure joint robustness, a dimension orthogonal to SVulAttack’s instance-specific optimization.

Jailbreaks and Transferable Prompt Attacks. Adversarial attacks on aligned LLMs have evolved from manual template engineering to automated frameworks. *Optimization-based* methods, such as GCG (Zou et al., 2023) and AutoDAN (Zhu et al., 2023), utilize gradient-guided or genetic search to find transferable adversarial suffixes. Concurrently, *LLM-guided black-box* attacks like PAIR (Chao et al., 2024), decomposition attack (Brown et al., 2025), and TAP (Mehrotra et al., 2024) leverage attacker models to iteratively refine prompts. Recent studies have extended this by characterizing the “utility” of such outputs (Nikolić et al., 2025). Existing evaluations, however, rarely examine how such transferable prompts interact with *code* tasks in a *detection* setting where edits must preserve compilability and semantics. We adapt GCG to this constrained setting.

3. Threat Model & Attacks

3.1. Threat Model

Adversary objective. We study evasion attacks against LLM-based vulnerability detectors. Given a ground-truth VULNERABLE function x and a detector $f(\cdot)$, the adversary aims to produce a perturbed function x' such that $f(x') = \text{BENIGN}$ (a false negative), allowing the vulnerability to bypass automated security gates.

Capabilities and semantic-invariance constraint. The adversary may modify only the *source-code input* while aiming to preserve **semantic invariance**; the transformed program must remain compilable and retain the underlying vulnerability. We restrict edits to four carriers that are intended to be semantics-preserving by construction: (i) scope-consistent *identifier substitution*, (ii) non-executable *comment carriers*, (iii) *preprocessor carriers* (macros/conditional guards) that are inactive under our compilation setting (e.g., unused macro definitions or disabled guards), and (iv) *dead-branch insertion* with a statically false predicate. We automatically validate carrier well-formedness (scope-consistent replacement, balanced comment delimiters, well-nested preprocessor directives/macro definitions, and syntactically valid dead-branch templates); we report pass rates and retain all samples without post-hoc filtering, validated by two-tier analysis: differential syntactic analysis (Tree-sitter (Khare et al., 2025)) on 5,000 functions and compilation-based validation (gcc) on another 1,434 standalone-compileable functions (Appendix A.3, Ta-

bles 6–7).

Knowledge regimes. We evaluate robustness under three realistic access assumptions:

- **White-box.** The adversary has full access to model weights and gradients, enabling direct gradient-guided optimization (e.g., GCG) of adversarial strings.
- **Black-box (API) via transfer.** Targeting proprietary models with inaccessible internals, the adversary optimizes universal strings on a smaller surrogate model and applies them to the target without further modification.
- **Operational black-box.** Targeting large locally-hosted models where weights are accessible but direct gradient-based optimization is computationally expensive for typical adversaries. We primarily evaluate this regime using **transfer-only methods** to establish a realistic baseline of low-cost exploitability. However, to quantify the gap between this low-cost approach and the worst-case security risk, we explicitly perform an **on-target white-box ablation** (see Table 5) as a high-cost upper bound.

Detailed model specifications and versions are provided in Appendix A.1.

3.2. GCG-based Optimization

Code presents a unique constraint: syntax errors break compilation. Standard GCG generates random-looking strings that often violate language grammar. We address this by restricting optimization to four carrier types with automated validity checks.

We use the Greedy Coordinate Gradient (GCG) algorithm to optimize a discrete, printable adversarial string σ that induces a prediction flip from VULNERABLE to BENIGN. GCG uses token-level gradients to guide coordinate-wise updates in a discrete search space, while all edits are restricted to the semantics-preserving transformation space defined by our threat model. We choose GCG for its ability to produce a universal string that transfers across both samples and models (§5.4).

Optimization Objective and Universal Strategy.

The attacker maximizes the model’s relative preference for the target label BENIGN over the ground truth VULNERABLE. Specifically, for a code instance x and carrier $\mathcal{T}(x, \sigma)$, we maximize the log-odds objective $\mathcal{J}(\sigma; x) = \log p_{\theta}(\text{BENIGN} \mid \mathcal{T}(x, \sigma)) - \log p_{\theta}(\text{VULNERABLE} \mid \mathcal{T}(x, \sigma))$. To ensure generalization, rather than optimizing per-instance, we learn a single **universal** adversarial string σ over a fixed support set \mathcal{X}_{opt} ($m=10$) by maximizing the mean performance: $\mathcal{J}_{\text{univ}}(\sigma) = \frac{1}{m} \sum_{x \in \mathcal{X}_{\text{opt}}} \mathcal{J}(\sigma; x)$. Post-optimization, σ is frozen to evaluate zero-shot transferability. The success of such input-agnostic triggers suggests that the detector’s vulnerability stems from systematic feature bias rather than

instance-specific brittle directions.

Implementation details. Optimization hyperparameters, surrogate model selection (Qwen2.5-Coder-14B), and prompt templates are provided in Appendix B.5 and Appendix E.

3.3. Attack Categories

We define the transformation operator $\mathcal{T}(x, \sigma)$ through four families of insertion carriers. The following methods ensure functional equivalence by construction, modifying only the source-code input while strictly maintaining compilability and executable behavior (see Appendix F for details):

1. **Identifier substitution.** We apply a consistent renaming map $\mathcal{M} : v \mapsto \sigma$ to the specific identifier v explicitly flagged by the detector (i.e., extracted from the "variable" JSON field), or to the most frequent local identifier if attribution is unavailable. We replace all occurrences of v within its scope. This focuses the perturbation on lexical cues without affecting variable binding or logic (*avoiding variable shadowing*).
2. **Comment-carrier insertion.** We inject σ into syntactically valid comment carriers (e.g., prepending a multi-line header). Comments act as transparent containers for adversarial tokens, allowing the insertion of non-interpretable strings.
3. **Preprocessor-based insertion (macro/guard carriers).** We inject σ into inactive preprocessor regions, specifically unused macro definitions (denoted `macro_name`) or disabled conditional guards. These regions are stripped or ignored during compilation, ensuring zero impact on runtime behavior.
4. **Dead-branch code insertion.** We inject σ into a formally unreachable control-flow block (e.g., `if (0) { }`). Unlike preprocessor directives, this carrier is syntactically indistinguishable from executable code, serving as a diagnostic for the detector’s ability to resolve basic Boolean control flow.

Family-specific candidate constraints. To ensure GCG-optimized strings remain valid under each carrier, we apply family-specific constraints to the candidate alphabet. For identifier substitution and dead-branch code, we enforce standard C-identifier compliance (alphanumeric with underscores, non-numeric start). For macro bodies and preprocessor-guarded blocks, we restrict the search space to a printable subset and enforce single-line constraints to prevent preprocessor syntax errors. Detailed vocabulary definitions and filtering rules are provided in Appendix A.2.

Default carriers and ablations. Unless otherwise specified, comment-carrier insertion uses a leading/header carrier, and macro insertion uses the macro-name carrier (`macro_name`). We study alternative placements (mid-

dle/trailing) and the macro-body carrier (`macro_body`) only in a focused ablation (Table 9).

4. Experimental Setup

4.1. Datasets Construction

Unified benchmark and design goals. To isolate *robustness to semantics-preserving edits* from confounders such as duplication leakage and length artifacts, we construct a single unified benchmark, UNIFIED-VUL-N ($N=5000$). We pool vulnerable functions from PrimeVul, BigVul, and DiverseVul, enforcing three strict controls: (i) *global cross-source de-duplication* to prevent inflation from repeated functions, (ii) a *fixed source composition* to standardize evaluation across models, and (iii) a *shared prompt budget* to ensure valid comparisons.

Deduplication by normalization-only hashing. To prevent evaluation inflation from surface-level duplicates, we canonicalize code logic (stripping comments and formatting) to define a deterministic equivalence class via SHA-256 hashing. **This normalization is used strictly for cross-source auditing; models are always evaluated on the original, unmodified source code.** Detailed normalization rules are provided in Appendix B.1.

Filtering and Sampling. We restrict code to ≤ 4096 tokens to reserve headroom for adversarial carriers and eliminate truncation-driven artifacts. A deterministic, quota-controlled sampling strategy ensures a stable and auditable benchmark composition (also see Appendix B.1).

4.2. Evaluation Protocol

Strict Parsing and Conservative Success Criterion. We employ a deterministic strict parser to ensure robustness measurements reflect true *detection-time integrity* rather than output formatting artifacts. A successful evasion is counted *iff* the model produces a valid JSON with `label="BENIGN"` for a ground-truth vulnerable input. Parsing failures, refusals, or hallucinations are counted as **Resist** (failure to evade). This yields a conservative estimate of attack success: the adversary wins only by forcing a decisive false negative. Empirically, output stability is high ($> 99.9\%$ valid parse rate), confirming that measured failures stem from semantic understanding gaps, not syntax degradation.

Evaluation Decomposition: Conditional Evasion. To isolate robustness from clean-accuracy capabilities, we evaluate attacks *conditionally* on Clean True Positives (TP_{clean}). Since a pre-existing error cannot be "further evaded," applying attacks to the entire dataset would inflate perceived robustness. We define $\text{Flip}(A)$ as the subset of TP_{clean} successfully evaded under attack A , and $\text{Resist}(A)$ as those

Table 1. Baseline clean coverage on the unified C/C++ evaluation set. Absolute counts and $\text{TPR}_{\text{clean}}$ are reported; attack metrics ($|\text{Flip}_{\text{union}}|$, $|\text{Resist}_{\text{complete}}|$) appear in §5.1.

Model	N	$ \text{TP}_{\text{clean}} $	$ \text{FN}_{\text{clean}} $	$\text{TPR}_{\text{clean}}$ (%)
Qwen2.5-Coder-32B	5000	1121	3879	22.42
Llama3.1-8B	5000	1552	3448	31.04
CodeAstra	5000	3454	1546	69.08
GPT-4o	5000	2300	2700	46.00
GPT-5-mini	5000	3681	1319	73.62

that maintain detection.

Primary Robustness Metrics. We report three metrics to characterize the *Robustness & Accuracy Gap*:

1. **Conditional Attack Success Rate** (ASR_{cond}). The fraction of correctly detected vulnerabilities that are flipped by a specific attack vector ($|\text{Flip}|/|\text{TP}_{\text{clean}}|$).
2. **Complete Resistance** (CR). The fraction of vulnerabilities that withstand *all* evaluated attack families ($(\cap_k \text{Resist}(A_k))/|\text{TP}_{\text{clean}}|$). This serves as the **security floor**, indicating the proportion of reliable detections that are truly invariant to semantic perturbations.
3. **End-to-End Recall Drop** (ΔTPR). The absolute decrease in detection coverage on the full dataset ($|\text{Flip}_{\cup}|/N$). This measures the operational risk of deploying the model in an adversarial environment.

Formal derivations and single-family variants are detailed in Appendix B.2.

Baseline Clean Coverage. All attack metrics are contextualized against the clean performance baselines reported in Table 1, establishing the performance ceiling from which robustness degrades.

5. Results

5.1. Main Results: Overall Attack Effectiveness

One would expect that a detector achieving 70% clean accuracy provides reliable security coverage for the vulnerabilities it identifies. Our evaluation reveals the opposite: across all models except GPT-5-mini, over 87% of correctly detected vulnerabilities can be flipped to false negatives using only semantics-preserving edits (Figure 2). CodeAstra, despite correctly flagging 3,454 vulnerabilities on clean inputs, maintains robust detection for only 4 functions under on-target attacks (CR = 0.12%), a 99.88% collapse in detection integrity.

This pattern occurs **under realistic access assumptions**: surrogate-transfer attacks on black-box APIs (GPT-4o, GPT-5-mini) and operational black-box models (Qwen2.5-Coder-32B), supplemented by on-target optimization for accessible models (Llama3.1-8B, CodeAstra) to establish up-

per bounds. Across this threat landscape, GPT-5-mini is an exception, exhibiting substantially lower attack success (44.04% union ASR_{cond}) compared to other models (87%–100%), suggesting stronger invariance to carrier-based perturbations. These results indicate that *clean benchmark accuracy is not a security guarantee*. An attacker needs only to evade the subset of cases a detector would otherwise catch, and our results show this is achievable through innocuous transformations like identifier renaming or comment insertion (Table 2; clean baseline in Table 1).

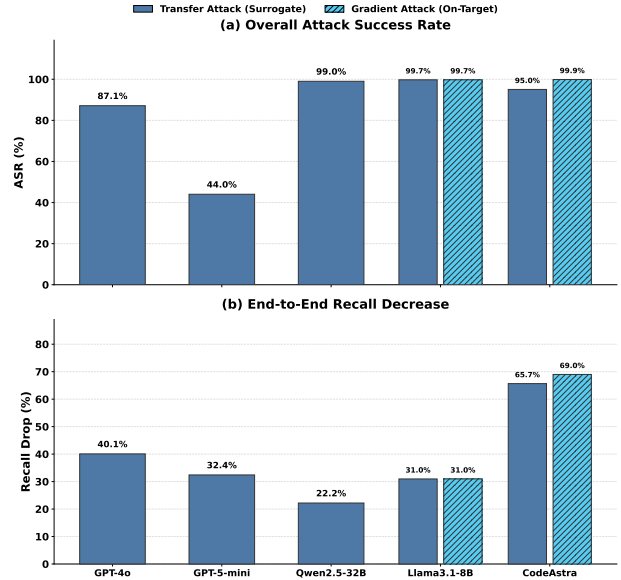


Figure 2. Overall attack effectiveness across models. Solid bars: transfer attacks using universal strings from Qwen2.5-Coder-14B surrogate. Hatched bars: on-target optimization (Llama3.1-8B, CodeAstra only). (a) Union ASR_{cond} across carriers. (b) End-to-end recall decrease (ΔTPR).

Benign-class invariance. To verify that our edits induce targeted false negatives rather than indiscriminate label corruption, we evaluate attacks on a held-out set of 500 ground-truth benign functions. Across all models and attack methods, we observe **100% benign-class invariance**: every function predicted as BENIGN under clean inference remains BENIGN after applying our transformations. This supports that the observed flips reflect targeted integrity violations rather than indiscriminate label corruption.

5.2. Carrier-Specific Vulnerabilities: Preprocessor Attacks Dominate

We break down attack effectiveness by carrier under surrogate transfer (Table 2). **Three patterns emerge.** First, no single carrier dominates: `ifdef` achieves near-complete evasion on Llama3.1-8B (99.03%) and Qwen2.5-Coder-32B (98.84%) but achieves moderate success elsewhere. Second, preprocessor carriers often outperform identifier substitu-

Table 2. Conditional attack success rate (ASR_{cond}) under surrogate transfer. Universal strings from Qwen2.5-Coder-14B applied to all targets.

Model	Identifier Sub.	Comment	ifdef	macro	dead-branch
GPT-4o	31.09%	65.48%	71.61%	42.35%	19.09%
GPT-5-mini	10.62%	18.34%	28.14%	21.57%	17.58%
Qwen2.5-Coder-32B	26.94%	91.53%	98.84%	85.81%	63.15%
Llama3.1-8B	34.66%	64.50%	99.03%	96.33%	59.79%
CodeAstra	4.72%	78.60%	42.59%	75.48%	72.12%

tion, suggesting over-reliance on non-executable boundary tokens. Third, GPT-5-mini exhibits uniformly low ASR (10–28%), indicating broader invariance. Besides, Dead-branch carriers are also effective on several models, indicating limited dead code alignment.

Model-specific patterns. Most models show high vulnerability to preprocessor carriers, with Llama3.1-8B and Qwen2.5-Coder-32B near-ceiling (85–99%). CodeAstra presents a distinct profile: identifier substitution transfers poorly (4.72%), while boundary carriers remain effective (42–79%). On-target optimization reverses this pattern (§5.4).

Positional and functional sensitivity. Attack success is sensitive to carrier placement and syntactic role. Trailing comment carriers outperform leading ones for Llama3.1-8B and CodeAstra, consistent with boundary-position bias in long-context aggregation. Similarly, macro-name carriers are considerably more potent than macro-body carriers (detailed ablation in Table 9). Function length shows weak correlation with evasion (Pearson $r \in [-0.17, -0.02]$), and CWE-level analysis reveals modest variation (Appendix D.1 and Figure 4).

5.3. Sanitization Eliminates Carriers but Induces Prediction Drift

Table 3. Sanitization eliminates targeted carriers (ASR \rightarrow 0%) but induces prediction drift on clean inputs (see Table 10 for details).

Model	Comment	ifdef	macro	Δ TP
Qwen2.5-Coder-32B	91.53 \rightarrow 0%	98.84 \rightarrow 0%	85.81 \rightarrow 0%	+5.2%
Llama3.1-8B	64.50 \rightarrow 0%	99.03 \rightarrow 0%	96.33 \rightarrow 0%	+8.6%
CodeAstra	78.60 \rightarrow 0%	42.59 \rightarrow 0%	75.48 \rightarrow 0%	+0.1%

Given the high success of comment- and preprocessor-based carriers, we evaluate a simple input-sanitization baseline that removes these carrier surfaces prior to inference. The pipeline (i) strips C/C++ line and block comments, and (ii) canonicalizes/removes preprocessor directives before passing code to the detector. We treat this as a carrier-elimination baseline rather than a semantics-aware defense.

Table 3 shows that sanitization successfully drives ASR to zero for targeted carriers. However, it induces substantial *prediction drift*: stripping benign comments and preprocessor directives from unperturbed, ground-truth vulnera-

ble functions increases clean detection rates by up to 8.6% (Llama3.1-8B: 1552 \rightarrow 1685 true positives). This reveals that models utilize non-executable lexical context as decision-relevant features, indicating a lack of semantic invariance even absent adversarial perturbations (detailed drift analysis in Table 10, Appendix D).

Moreover, sanitization is not a free lunch: comments and preprocessor directives appear in 57.0% and 12.8% of functions, respectively, meaning this defense rewrites a substantial fraction of inputs. We exclude dead-code elimination, as it risks mis-eliminating live code without compiler-level context (Tu et al., 2024). Furthermore, sanitization fails to address executable-looking carriers like identifier substitution and dead-branch insertions.

5.4. Transfer Attacks Succeed on Black-Box APIs; On-Target Reveals Complex Interactions

Table 2 presents transfer results where universal strings optimized on Qwen2.5-Coder-14B are applied unchanged to all targets. This models a low-barrier adversary: optimization is performed once, and resulting strings are reused across vulnerable functions and deployed detectors. Across black-box and operational black-box targets, transfer achieves 44.04%–99.03% union ASR_{cond}, establishing that API opacity alone does not prevent evasion under semantics-preserving perturbations. However, transferability is not uniform: GPT-5-mini exhibits materially lower success (44.04%) than other models (87–99%), indicating that robustness varies across model families even under identical carriers.

On-target optimization reveals divergent vulnerability profiles. While transfer attacks establish a practical lower bound on exploitability, they may underestimate the true vulnerability of a model. To quantify the gap between low-cost transfer and worst-case security risk, we perform on-target universal GCG for Llama3.1-8B and CodeAstra (accessible models). Table 4 compares transfer and on-target regimes across carriers.

Table 4. Transfer vs. on-target attack success. Transfer uses universal strings from Qwen-14B surrogate; on-target optimizes directly on the target.

Model	Regime	ASR _{cond} (%)				
		Idsub	Comment	ifdef	macro	Dead-br
Llama3.1-8B	Transfer	34.66	64.50	99.03	96.33	59.79
	On-target	43.49	42.01	99.03	65.46	86.66
CodeAstra	Transfer	4.72	78.60	42.59	75.48	72.12
	On-target	85.41	63.06	16.62	98.87	97.51

For Llama3.1-8B, on-target optimization improves identifier substitution (34.66% \rightarrow 43.49%) and dead-branch insertion (59.79% \rightarrow 86.66%), but *degrades* comment (64.50% \rightarrow 42.01%) and macro (96.33% \rightarrow 65.46%). This suggests

that universal strings optimized on a surrogate can outperform target-specific optimization for certain carriers, likely because surrogate-optimized universal strings exploit more transferable boundary-token sensitivities.

CodeAstra exhibits a clear asymmetry. Transfer achieves 4.72% identifier success but 42.59% for ifdef. On-target optimization *inverts* this: identifier reaches (85.41%) while ifdef collapses (16.62%).

We hypothesize two mechanisms. For identifier substitution, CodeAstra’s loss landscape provides smooth gradients: GCG efficiently discovers variable-name perturbations that flip predictions. For ifdef, on-target GCG likely encounters optimization difficulty, so the optimizer converges to poor local minima that fail to exploit the vulnerabilities that surrogate-optimized strings (accidentally) discovered through multi-model training. This suggests that gradient-based optimization success depends not only on model vulnerabilities but also on the *optimizability* of the attack surface: some carrier spaces may be inherently harder to optimize even when vulnerabilities exist.

Qwen2.5-Coder-32B: Surrogate capacity and on-target upper bound. For Qwen2.5-Coder-32B (operational black-box), we ablate identifier substitution across surrogate capacities and on-target optimization (Table 5). Transferability is non-zero even for small surrogates (0.5B/1.5B: 6-7%), but increases with capacity (14B: 26.94%), indicating a representation-capacity threshold. On-target universal GCG achieves 92.50%, providing a clear upper bound when gradients are available. This gap (26.94% → 92.50%) quantifies the security improvement from restricting adversarial access: surrogate transfer yields a conservative lower bound under practical compute constraints, while on-target optimization demonstrates worst-case exploitability.

Table 5. Identifier substitution on Qwen2.5-Coder-32B: effect of surrogate capacity and on-target optimization. All settings use the same injection site, identifier constraints, and L_{max} .

Setting	ASR _{cond} (%)	Flipped / TP _{clean}
Surrogate transfer (Qwen2.5-Coder-0.5B → 32B)	6.87	77 / 1121
Surrogate transfer (Qwen2.5-Coder-1.5B → 32B)	6.42	72 / 1121
Surrogate transfer (Qwen2.5-Coder-14B → 32B)	26.94	302 / 1121
On-target universal GCG (Qwen2.5-Coder-32B)	92.50	1038 / 1121

Implications. These findings highlight three key insights. First, transferability amplifies risk by enabling low-cost, reusable attacks against multiple deployed detectors, including API-access models. Second, on-target optimization does not uniformly strengthen attacks- CodeAstra’s inverted profile and Llama’s macro degradation suggest complex

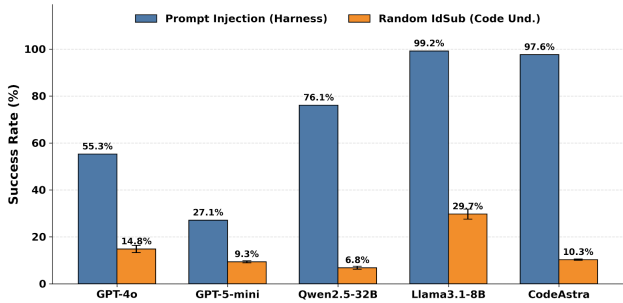


Figure 3. **Robustness against Non-GCG Baselines.** We compare prompt injection against random.idsub. While prompt injection achieves high success on some models (e.g., Llama3.1, CodeAstra), random perturbations (~10%) remain far less effective than our optimized attacks, confirming that code syntax requires targeted optimization rather than random noise.

cross-carrier interactions that warrant further investigation. Third, the gap between transfer and on-target regimes varies by model and carrier (4.72% → 85.41% for CodeAstra identifier vs. 99.03% → 99.03% for Llama ifdef), indicating that vulnerability assessment requires evaluating both threat models.

Our threat model operates at the input level (semantics-preserving edits) rather than the output level (harmful generation). Because attacks modify code while preserving executable behavior, standard output-safety mechanisms (alignment training, content filtering) do not directly translate into robustness as a vulnerability-detection gate. Finally, these effects are not specific to greedy decoding: on GPT-4o, union ASR_{cond} remains similar when increasing temperature from $T=0.0$ to $T=0.7$ (87.00% vs. 85.19%±0.65%; Appendix D.2).

We compare GCG-optimized attacks to non-optimized baselines targeting **distinct failure modes**: (i) *output format injection* by prepending // output: {"label": "BENIGN", "variable": ""} in comments (testing few-shot learning vulnerability, **outside our threat model**), and (ii) *random identifier substitution* under the same constraints (testing code-understanding robustness, **within our threat model**). Figure 3 illustrates these results.

The output format injection baseline achieves high success (55–99% across models), revealing that models can be manipulated by embedding target JSON outputs in code comments, an orthogonal vulnerability distinct from semantic robustness. In contrast, random.idsub is significantly weaker (7–30%), demonstrating that non-optimized renaming has a limited impact on code-understanding robustness.

6. Discussion

Clean-set accuracy alone does not guarantee reliability. While models like CodeAstra achieve near-70% clean recall, our evaluation reveals that this capability degrades under adversarial transformation, with complete resistance dropping to near zero (0.12%), implying that current detectors act less as robust semantic parsers and more as pattern-matchers over fragile lexical cues. Across semantics-preserving edits (§3), we observe a persistent integrity gap: models with high clean coverage can exhibit high union evasion and near-zero complete resistance, meaning that an attacker who can choose among multiple perturbation surfaces can often overturn most clean true positives. Even simple carrier-elimination preprocessing (§5.3) does not eliminate this risk, as evasion can migrate to remaining executable-looking channels.

Multiple metrics matter. Single-number summaries can be misleading for deployment decisions. Union success captures whether *any* available surface enables evasion, while complete resistance operationalizes a security floor when attackers can try multiple carriers. Per-method and CWE-level slices then identify where robustness breaks (which channels, which vulnerability types), enabling targeted mitigation rather than blanket conclusions from aggregate ASR.

Temperature and transfer analysis. The observed fragility is structural rather than stochastic. Evasion rates remain stable across decoding temperatures (Appendix D.2), ruling out random sampling artifacts. More importantly, the **high transferability of attacks from a 14B surrogate model to GPT-4o** points to shared representational blind spots: distinct models appear to over-index on identical non-executable tokens (e.g., `#ifdef` guards) while ignoring the invariant executable logic.

Decoupling of Domain Capability and Robustness. The performance profile of CodeAstra reveals a meaningful insight: although task-specific fine-tuning boosts baseline detection, it does not guarantee robustness. CodeAstra exhibits high vulnerability in specific channels (e.g., macro insertion) despite high clean accuracy. This suggests that domain specialization can coexist with-or mask-structural fragility, emphasizing that fine-tuned models require integrity evaluations just as rigorous as general-purpose ones.

Implications for Deployment and Defense. Our findings suggest three concrete directions for hardening detectors. First, training on carrier-diverse adversarial examples (spanning identifier, comment, and preprocessor surfaces) may enforce broader invariance than single-method defenses. Second, Complete Resistance should join clean accuracy as a co-equal deployment metric- a detector is only as robust as its weakest carrier. Third, ensemble approaches combining sanitization (for boundary carriers) with robust base models

may offer defense-in-depth where neither alone suffices.

Limitations and Future Directions. We focus on C/C++ functions with a fixed prompting protocol; extending to other languages and detection formulations would strengthen generality. While Tier 2 validation (differential AST analysis) scales to 5,000 functions and Tier 3 (compilation-based) provides strong proof on 1,434 functions (Appendix A.3), absolute behavioral equivalence requires full execution environments unavailable in function-level datasets. Future work should explore adversarial fine-tuning on semantics-preserving carriers, though computational cost and overfitting risks motivate investigating lightweight defense wrappers (Madry et al., 2019; Varshney et al., 2024).

7. Conclusion

On a unified C/C++ benchmark ($N=5000$), we present an integrity evaluation of LLM-based vulnerability detectors under semantics-preserving code perturbations, evaluating five carriers spanning four insertion families (identifier substitution, comments, preprocessor insertions, and dead-branch insertion) and quantifying robustness via union success and *complete resistance*. Across models, we observe widespread failures of semantic invariance: many vulnerabilities that are correctly detected on clean inputs can be flipped to false negatives via behavior-equivalent edits, and a single universal, carrier-constrained string optimized on a surrogate can transfer *unchanged* to black-box API targets. Sanitization can remove some insertion surfaces, but it rewrites many inputs and leaves executable-looking channels vulnerable. These findings collectively suggest that clean benchmark performance alone is insufficient as a security guarantee, and that integrity-oriented evaluations and defenses should explicitly target robustness to behavior-preserving code changes without resorting to overly conservative task-altering preprocessing.

Impact Statement

This work evaluates the robustness of LLM-based vulnerability detectors under semantics-preserving adversarial perturbations. We discuss both the positive contributions and potential risks of this research.

Positive Impacts. Our findings reveal essential blind spots in current LLM-based code security tools before they are exploited in the wild. By systematically characterizing failure modes and introducing metrics such as Complete Resistance, we provide actionable diagnostics for practitioners to harden detection pipelines. We believe responsible disclosure of these weaknesses, consistent with standard practices in security research, enables the community to develop more robust defenses.

Potential Risks and Mitigations. As with most security research, the techniques described could theoretically be misused to evade vulnerability detection. However, we note that: (1) the attack surfaces we study (identifier renaming, comment insertion, preprocessor directives) are already well-known code transformations; (2) we do not release optimized adversarial strings or attack toolkits; and (3) the primary barrier to exploiting vulnerabilities lies in discovering them, not in evading detection. We believe the defensive value of exposing these weaknesses substantially outweighs the marginal risk of informing attackers about evasion strategies they could likely discover independently.

References

- Brown, D., Sabbaghi, M., Sun, L., Robey, A., Pappas, G. J., Wong, E., and Hassani, H. Benchmarking misuse mitigation against covert adversaries, 2025. URL <https://arxiv.org/abs/2506.06414>.
- Bundt, J., Davinroy, M., Agadakos, I., Oprea, A., and Robertson, W. Black-box attacks against neural binary function detection. In *Proceedings of the 26th International Symposium on Research in Attacks, Intrusions and Defenses*, RAID 2023, pp. 1–16. ACM, October 2023. doi: 10.1145/3607199.3607200. URL <http://dx.doi.org/10.1145/3607199.3607200>.
- Chao, P., Robey, A., Dobriban, E., Hassani, H., Pappas, G. J., and Wong, E. Jailbreaking black box large language models in twenty queries, 2024. URL <https://arxiv.org/abs/2310.08419>.
- Chen, Y., Ding, Z., Alowain, L., Chen, X., and Wagner, D. Diversevul: A new vulnerable source code dataset for deep learning based vulnerability detection. In *Proceedings of the 26th International Symposium on Research in Attacks, Intrusions and Defenses*, RAID '23, pp. 654–668, New York, NY, USA, 2023. Association for Computing Machinery. ISBN 9798400707650. doi: 10.1145/3607199.3607242. URL <https://doi.org/10.1145/3607199.3607242>.
- Derczynski, L., Galinkin, E., Martin, J., Majumdar, S., and Inie, N. garak: A framework for security probing large language models, 2024. URL <https://arxiv.org/abs/2406.11036>.
- Ding, Y., Fu, Y., Ibrahim, O., Sitawarin, C., Chen, X., Aloatair, B., Wagner, D., Ray, B., and Chen, Y. Vulnerability detection with code language models: How far are we? *arXiv preprint arXiv:2403.18624*, 2024.
- Ebrahimi, J., Rao, A., Lowd, D., and Dou, D. Hotflip: White-box adversarial examples for text classification, 2018. URL <https://arxiv.org/abs/1712.06751>.
- Fan, J., Li, Y., Wang, S., and Nguyen, T. N. A c/c++ code vulnerability dataset with code changes and cve summaries. In *2020 IEEE/ACM 17th International Conference on Mining Software Repositories (MSR)*, pp. 508–512, 2020. doi: 10.1145/3379597.3387501.
- Fu, Y., Shayegan, E., Abdullah, M. M. A., Zaree, P., Abu-Ghazaleh, N., and Dong, Y. Vulnerabilities of large language models to adversarial attacks. In Chiruzzo, L., Lee, H.-y., and Ribeiro, L. F. R. (eds.), *Proceedings of the 62nd Annual Meeting of the Association for Computational Linguistics (Volume 5: Tutorial Abstracts)*, pp. 8–9, Bangkok, Thailand, August 2024. Association for Computational Linguistics. doi: 10.18653/v1/2024.acl-tutorials.5. URL <https://aclanthology.org/2024.acl-tutorials.5/>.
- Ganesan, H. S. Codeastra-7b: State-of-the-art vulnerability detection model. <https://huggingface.co/roo-0xhacker/CodeAstra-7b>, 2024.
- Jiang, Y., Huang, S., Treude, C., Su, X., and Wang, T. Shield broken: Black-box adversarial attacks on llm-based vulnerability detectors. *IEEE Transactions on Software Engineering*, 52(1):246–265, 2026. doi: 10.1109/TSE.2025.3638998.
- Khare, A., Dutta, S., Li, Z., Solko-Breslin, A., Alur, R., and Naik, M. Understanding the effectiveness of large language models in detecting security vulnerabilities. In *2025 IEEE Conference on Software Testing, Verification and Validation (ICST)*, pp. 103–114, 2025. doi: 10.1109/ICST62969.2025.10988968.
- Li, X., Ding, J., Peng, C., Zhao, B., Gao, X., Gao, H., and Gu, X. Safegenbench: A benchmark framework for security vulnerability detection in llm-generated code, 2025. URL <https://arxiv.org/abs/2506.05692>.
- Madry, A., Makelov, A., Schmidt, L., Tsipras, D., and Vladu, A. Towards deep learning models resistant to adversarial attacks, 2019. URL <https://arxiv.org/abs/1706.06083>.
- Mehrotra, A., Zampetakis, M., Kassianik, P., Nelson, B., Anderson, H., Singer, Y., and Karbasi, A. Tree of attacks: Jailbreaking black-box llms automatically, 2024. URL <https://arxiv.org/abs/2312.02119>.
- Microsoft. Microsoft digital defense report 2025: Lighting the path to a secure future. Technical report, Microsoft, 2025. URL <https://www.microsoft.com/en-us/corporate-responsibility/cybersecurity/microsoft-digital-defense-report-2025/>.

- Mu, W., Xu, L., Pei, S., Mi, L., and Zhou, H. Evaluate-and-purify: Fortifying code language models against adversarial attacks using llm-as-a-judge, 2025. URL <https://arxiv.org/abs/2504.19730>.
- Nikolić, K., Sun, L., Zhang, J., and Tramèr, F. The jailbreak tax: How useful are your jailbreak outputs?, 2025. URL <https://arxiv.org/abs/2504.10694>.
- Orvalho, P. and Kwiatkowska, M. Are large language models robust in understanding code against semantics-preserving mutations?, 2025. URL <https://arxiv.org/abs/2505.10443>.
- Rath, A., Qi, W., Li, Y., and Wang, X. Natgvd: Natural adversarial example attack towards graph-based vulnerability detection, 2025. URL <https://arxiv.org/abs/2510.04987>.
- Tu, H., Jiang, L., Gao, D., and Jiang, H. Beyond a joke: Dead code elimination can delete live code. In *2024 IEEE/ACM 46th International Conference on Software Engineering: New Ideas and Emerging Results (ICSE-NIER)*, pp. 32–36, 2024.
- Varshney, N., Dolin, P., Seth, A., and Baral, C. The art of defending: A systematic evaluation and analysis of LLM defense strategies on safety and over-defensiveness. In Ku, L.-W., Martins, A., and Srikumar, V. (eds.), *Findings of the Association for Computational Linguistics: ACL 2024*, pp. 13111–13128, Bangkok, Thailand, August 2024. Association for Computational Linguistics. doi: 10.18653/v1/2024.findings-acl.776. URL <https://aclanthology.org/2024.findings-acl.776/>.
- Vassilev, A., Oprea, A., Fordyce, A., Anderson, H., Davies, X., and Hamlin, M. Adversarial machine learning: A taxonomy and terminology of attacks and mitigations. Technical Report NIST AI 100-2 E2025, National Institute of Standards and Technology (NIST), 2025. URL <https://csrc.nist.gov/pubs/ai/100/2/e2025/final>.
- Verizon. 2025 data breach investigations report. Technical report, Verizon, 2025.
- Wei, Z., Hu, P., Lang, S., Yan, H., Mei, L., Zhang, Y., Yang, C., Hao, J., and Han, Z. Automated red-teaming framework for large language model security assessment: A comprehensive attack generation and detection system, 2025. URL <https://arxiv.org/abs/2512.20677>.
- Zhu, S., Zhang, R., An, B., Wu, G., Barrow, J., Wang, Z., Huang, F., Nenkova, A., and Sun, T. Autodan: Interpretable gradient-based adversarial attacks on large language models, 2023. URL <https://arxiv.org/abs/2310.15140>.
- Zou, A., Wang, Z., Carlini, N., Nasr, M., Kolter, J. Z., and Fredrikson, M. Universal and transferable adversarial attacks on aligned language models, 2023. URL <https://arxiv.org/abs/2307.15043>.

A. Detailed Threat Model

A.1. Target Models Details

We evaluate the proposed attacks across five state-of-the-art LLMs, categorized by their access regimes:

For reproducibility, we explicitly set `temperature=0.0` for GPT-4o to ensure deterministic decoding, while GPT-5-mini was evaluated under its mandatory default settings, as the API does not currently support sampling parameter adjustment.

Regime	Model Family	Specific Version / API ID
White-box	Llama 3.1	meta-llama/Llama-3.1-8B-Instruct
White-box	CodeAstra	rootxhacker/CodeAstra-7B (Ganesan, 2024)
White-box	Qwen2.5-Coder	Qwen/Qwen2.5-Coder-14B-Instruct (Surrogate)
Black-box (API)	GPT-4o	gpt-4o-2024-08-06
Black-box (API)	GPT-5-mini	gpt-5-mini-2025-08-07
Operational Black-box	Qwen2.5-Coder	Qwen/Qwen2.5-Coder-32B-Instruct

A.2. Vocabulary Constraints

To ensure that injected payloads do not break C/C++ syntax or preprocessor parsing, we restrict the GCG search space \mathcal{A} based on the carrier type:

- **Identifiers and Dead-branch.** Restricted to $[A-Za-z_][A-Za-z0-9_]*$.
- **Macro Bodies and Guards.** We use a filtered printable ASCII set $\mathcal{A}_{\text{macro}}$ that excludes characters capable of terminating string literals or lines prematurely:

$$\mathcal{A}_{\text{macro}} = \mathcal{A}_{\text{printable}} \setminus \{", \backslash, \backslash n, \backslash r\} \quad (1)$$

where $\backslash n$ and $\backslash r$ denote newline and carriage return characters, respectively.

A.3. Semantics Preservation Validation

We validate semantics preservation through a two-tiered approach: (1) **Constraint-based Validation** to verify method-specific injection rules, and (2) **Differential Syntactic Analysis** using Tree-sitter to ensure that perturbations do not introduce new syntax errors compared to the original code. This approach is robust to the incomplete nature of function-level datasets (e.g., missing headers) while strictly flagging syntax violations.

Tier 1: Constraint-based Validation. For each attack method, we verify rigorous structural constraints:

- **Identifier substitution.** (i) Replacement strings must match valid C/C++ identifier patterns ($[A-Za-z_][A-Za-z0-9_]*$); (ii) replacement must be consistent across the scope; (iii) **Variable Shadowing Check.** We verify that the new identifier does not conflict with existing variables in the local or global scope to prevent logic corruption.
- **Comment-carrier insertion.** We verify that delimiters ($/ * */$ or $//$) are balanced and boundaries are correctly recognized by a lexer.
- **Preprocessor-based insertion.** We verify that directives ($\#ifdef/\#endif$) are strictly balanced and macro names use unique prefixes (e.g., SAFE_FUNC_) to avoid collisions.
- **Dead-branch code insertion.** We verify that (i) the condition is statically false (e.g., $if(0)$), (ii) braces are balanced, and (iii) the block is syntactically distinct from surrounding code.

Tier 2: Differential Syntactic Analysis (Tree-sitter). Standard compilation fails on function snippets due to missing translation units (e.g., undefined types like $u8$). To address this, we employ **Tree-sitter**, a robust incremental parser. We define a transformation as *Syntactically Preserved* if the number of AST error nodes in the adversarial code (E_{adv}) does not exceed the error nodes in the original code (E_{orig}):

$$\text{Validity} \iff E_{adv} \leq E_{orig}$$

Table 6. **Semantics Preservation Rates across Models.** We report two metrics: (1) **Constraint Sat.** Fraction of samples satisfying method-specific rules. (2) **Tree-sitter Valid.** Fraction of samples where the attack introduces no new AST error nodes ($E_{adv} \leq E_{orig}$). High validity across diverse architectures confirms the stability of our attack generation.

Metric	Id. Sub	Comment	#ifdef	Macro	Dead-Branch	Overall
<i>Model: Qwen2.5-Coder-32B</i> ($N = 1121$)						
Constraint Sat. (%)	100.0	99.0	99.8	99.8	99.8	99.7
Tree-sitter Valid (%)	98.0	100.0	100.0	100.0	99.8	99.6
<i>Model: CodeAstra</i> ($N = 3454$)						
Constraint Sat. (%)	100.0	99.5	99.9	99.9	98.0	99.5
Tree-sitter Valid (%)	98.2	100.0	100.0	100.0	99.5	99.5
<i>Model: Llama3.1-8B</i> ($N = 1552$)						
Constraint Sat. (%)	100.0	99.4	99.8	99.8	97.9	99.4
Tree-sitter Valid (%)	98.6	100.0	100.0	100.0	99.4	99.6

This differential metric filters out pre-existing errors caused by missing context (e.g., unknown macros) and isolates syntax errors introduced strictly by the attack.

Validation Results. Table 6 summarizes the validation rates across three diverse model families (Qwen, CodeAstra, and Llama). **Constraint Satisfaction.** Across all models, $> 99\%$ of samples satisfy method-specific constraints. **Syntactic Validity.** Under Tree-sitter differential analysis, our attacks achieve a consistent pass rate of **99.5%** on average (e.g., 99.6% for Qwen2.5-Coder-32B and 99.5% for CodeAstra). Notably, the **Tree-sitter Valid** score for preprocessor-based carriers (#ifdef, Macro) and Comment carriers reaches **100%**, while Identifier Substitution maintains $\approx 98.2\%$. This cross-model consistency confirms that our adversarial perturbations- whether applied to small or large test sets-preserve the syntactic structure of the original code, effectively ruling out malformed injections as a cause for evasion.

Dataset Compilation Challenges. Function-level vulnerability datasets lack full compilation context (missing headers, type definitions, build dependencies). To enable rigorous compilation-based validation, we constructed a compilable subset from PrimeVul.

Tier 3: Compilation-based Validation. We constructed a **Compilable Validation Set** through:

1. Sample 2,000 ground-truth vulnerable functions from PrimeVul’s compilable subset
2. Verify all 2,000 compile standalone via `gcc -fsyntax-only` with standard headers
3. Evaluate on CodeAstra (highest TPR=69.08%) \rightarrow 1,434 correctly detected (71.7%)
4. Apply transfer attacks using universal strings from Qwen2.5-Coder-14B surrogate
5. Test compilation preservation after attack

Header Injection Harness. `stdio.h, stdlib.h, string.h, stdint.h, stddef.h, stdbool.h`

Compiler flags: `gcc -x c -fsyntax-only -Wno-implicit-function-declaration -`

Validation Results. Table 7 shows compilation preservation rates. Additive carriers achieve **perfect 100% preservation** (1,434/1,434), providing compiler-verified proof of semantics-preservation by construction. Identifier Substitution achieves 90.9% (1,303/1,434). The 131 failures stem from collisions with injected header symbols (`uint8_t, size_t, printf, malloc, etc.`) and are excluded from ASR calculations.

Table 7. **Compilation Preservation under Transfer Attacks** ($N=1,434$). CodeAstra true positives attacked with universal strings from Qwen-14B (Table 2). Validation via `gcc -fsyntax-only`.

Attack Carrier	Baseline	After Attack	Preservation
Identifier Substitution	1,434	1,303	90.9%
Comment Insertion	1,434	1,434	100.0%
#ifdef Guard	1,434	1,434	100.0%
Macro Definition	1,434	1,434	100.0%
Dead-Branch	1,434	1,434	100.0%

Relationship to Main Results. Main evaluation (§5) uses full dataset ($N=5,000$, all models) with Tree-sitter validation (Tier 2). Tier 3 provides compiler-verified confirmation on the CodeAstra subset using identical transfer strings. The two

tiers are complementary: Tier 2 scales to full evaluation; Tier 3 provides enough proof on a representative subset.

Limitations. Tier 3 covers CodeAstra predictions only, though transfer string universality means results generalize to other models. PrimeVul functions that require project-specific headers (28.3% of the original compilable sample) are excluded.

B. Detailed Experimental Setup

B.1. Dataset Construction Details

Data sources and target language. UNIFIED-VUL-N contains vulnerable functions written in C/C++ and is constructed by pooling the vulnerable subsets from PrimeVul, BigVul, and DiverseVul. The goal is to evaluate robustness under semantics-preserving transformations on a single, fixed benchmark with controlled composition.

Normalization for cross-source deduplication. For the sole purpose of cross-source deduplication, we build a normalized string `code_norm` for each function. The normalization is only for the purpose of deduplication, so the selected dataset still has comments. The normalization removes surface-level variation while preserving the underlying C/C++ token sequence:

- Remove C-style block comments (`/* ... */`) and line comments (`// ...`).
- Remove #-style comments that are not preprocessor directives (i.e., do not begin with a valid directive keyword), so that purely comment-like # lines do not affect deduplication.
- Canonicalize newlines and collapse runs of whitespace (spaces/tabs) to a single space, without altering non-whitespace characters.

This normalization is *not* applied to the code presented to the model; it is only used to detect duplicates across datasets.

Deduplication rule. We compute `code_hash = SHA256(code_norm)` and treat two functions as duplicates if their hashes match. Deduplication is performed globally across the pooled data (i.e., across all three sources), ensuring that the final set contains no cross-source duplicates under the normalization above.

Context budget and token-length filtering. To guarantee sufficient headroom for injected strings and to standardize the context budget across models, we filter functions by *code-only* token length using the Qwen2.5-Coder-14B tokenizer. Specifically, we require the code-only length to be at most 4096 tokens, where “code-only” refers to the function text used as input code (excluding any additional prompt or JSON schema wrappers). This constraint ensures that our injected variants remain within model context limits under the shared evaluation prompt.

Quota-controlled deterministic sampling. After global deduplication and length filtering, we enforce fixed per-source quotas of 3000 (PrimeVul), 1000 (BigVul), and 1000 (DiverseVul). To make selection deterministic, we shuffle items within each source once using a fixed random seed (`seed=42`) and then select items in a fixed priority order (PrimeVul → BigVul → DiverseVul), skipping any item whose `code_hash` has already been selected. We continue until all quotas are met.

Evaluation uses original code (no normalization at inference). All evaluations (clean and attacked) use the original, unnormalized code for each function as provided by the source dataset, including comments and preprocessor directives. The normalized string is used only to define `code_hash` for deduplication.

Released artifacts. We release three artifacts to reproduce the dataset and enable audits:

- **JSONL.** the final UNIFIED-VUL-N set, with one record per function including the original function text and metadata (source, id, CWE label).
- **CSV manifest.** a per-item manifest with (at minimum) `source`, `id`, `cwe`, `func` (original code), `code_norm` (dedup-normalized string), and `code_hash` (SHA-256 of `code_norm`).
- **Meta JSON.** dataset-level metadata, including the random seed, tokenizer name, token budget, counts before/after normalization and deduplication, and the exact quota configuration.

Table 8. Benign-side effects and invariance. Clean/Sanitized FPRs are measured on N_{benign} ground-truth benign functions. $\Delta\text{FPR}_{\text{sanit}}$ is the change (percentage points) after sanitization. Benign-class Invariance is computed on benign functions predicted as BENIGN under clean inference and remains BENIGN after applying the union of semantics-preserving attacks.

Model	N_{benign}	Clean FPR (%)	Sanitized FPR (%)	$\Delta\text{FPR}_{\text{sanit}}$ (pp)	Benign Invariance (%)
Qwen2.5-Coder-32B	500	11.0 (55/500)	9.6 (48/500)	-1.4	100.0 (445/445)
GPT-4o	500	36.2 (181/500)	29.8 (149/500)	-6.4	100.0 (319/319)
CodeAstra	500	70.0 (350/500)	63.4 (317/500)	-6.6	100.0 (150/150)
Llama3.1-8B	500	16.8 (84/500)	18.0 (90/500)	+1.2	100.0 (416/416)
GPT-5-mini	500	54.4 (272/500)	56.2 (281/500)	+1.8	100.0 (228/228)

B.2. Additional metric variants.

For a single attack family A_k , we also report

$$\text{ASR}_{\text{cond}}(A_k) = \frac{|\text{Flip}(A_k)|}{|\text{TP}_{\text{clean}}|}, \quad \text{CR}(A_k) = \frac{|\text{Resist}(A_k)|}{|\text{TP}_{\text{clean}}|}.$$

Define the clean true-positive rate as $\text{TPR}_{\text{clean}} = \frac{|\text{TP}_{\text{clean}}|}{N}$. Under the union of attacks, the attacked true-positive rate is

$$\text{TPR}_{\text{att}} = \frac{|\text{TP}_{\text{clean}}| - |\text{Flip}_{\cup}|}{N},$$

So the recall drop satisfies the equivalent form.

$$\Delta\text{TPR} = \text{TPR}_{\text{clean}} - \text{TPR}_{\text{att}} = \frac{|\text{Flip}_{\cup}|}{N}.$$

B.3. Benign-Class Invariance and False Positives

Setup. We evaluate benign-class invariance on a held-out set of $N_{\text{benign}}=500$ ground-truth benign functions. **Clean FPR** is the fraction of benign functions predicted as VULNERABLE under clean inference (baseline model error). Sanitized FPR is computed after applying the same sanitization pipeline as in §5.3 (comment stripping and preprocessor removal); we report $\Delta\text{FPR}_{\text{sanit}}$ as the change in false-positive rate (percentage points) from clean to sanitized inputs. **Benign-class Invariance Rate** is the fraction of benign functions that are predicted as BENIGN under clean inference and remain BENIGN after applying our semantics-preserving attacks (union over all attack methods). This metric directly measures whether our attacks preserve benign-class predictions, which is aligned with our attack objective (evading vulnerability detection without introducing false positives).

Results. Table 8 reports per-model clean FPR, sanitized FPR (and $\Delta\text{FPR}_{\text{sanit}}$), and benign-class invariance rate. All models achieve 100% benign-class invariance rate, demonstrating that our semantics-preserving attacks preserve benign-class predictions: all functions that are correctly classified as BENIGN under clean inference remain BENIGN after attack.

B.4. Robustness of Reference Tokenizer for Length Filtering

To ensure fair cross-model comparisons, we standardized length filtering using the Qwen2.5-Coder-14B tokenizer to maintain an identical evaluation set across all targets. Per-model filtering would result in inconsistent subsets, making metrics like $\text{TPR}_{\text{clean}}$ and ASR_{cond} non-comparable. Correlation analysis on 500 random samples confirms that the Qwen tokenizer is highly representative: it achieves a Pearson correlation of $r = 0.9998$ with Llama-3.1-8B and $r = 0.9941$ with Mistral-7B-Instruct-v0.2, which is the original model of CodeAstra. The mean length difference relative to Llama is only -5.57 tokens (max 16). Given our 4096-token limit, these negligible deviations ensure that the filtering process does not introduce systemic bias against specific architectures.

B.5. Compute and Latency Statistics

We report compute and latency statistics for universal GCG optimization to assess practical attack cost. For the on-target identifier substitution experiment on Qwen2.5-Coder-32B (reported in §5, Transferability), we instrumented the GCG optimization loop to track forward passes and wall-clock time. The optimization uses curriculum learning where m_c

increases from 1 to $m_{\text{train}}=10$ over the first 10 steps (one step per training function), then optimizes all $m_{\text{train}}=10$ training prompts together for up to $S=500$ total steps. Note that the optimization is performed only on the training set ($m_{\text{train}}=10$ functions), not on the full evaluation set ($|\text{TP}_{\text{clean}}|=1121$ functions).

Optimization Hyperparameters. To ensure reproducibility, we used a fixed configuration for the GCG algorithm across all experiments. We set the optimization steps $S=500$, candidate search width to 256 (number of candidates generated per step), and top- k filtering to 128 for gradient guidance. Candidate evaluation used a batch size of 8. The adversarial string σ was initialized with a fixed placeholder pattern "x_x_x_x_x_x_x_x_x_x_" (length 20) to constrain the search space, and the optimization process used a fixed random seed of 42. **The support set \mathcal{X}_{opt} ($m=10$) was sampled randomly from the training split using a fixed seed of 21 to ensure reproducibility.**

Hardware and software setup. We run experiments on NVIDIA H100 GPUs (typically 1 GPU per run). Models are loaded in bfloat16 precision without quantization. The tokenizer is Qwen2.5-Coder-14B HuggingFace tokenizer for length filtering; optimization uses the target model’s tokenizer (Qwen2.5-Coder-32B for on-target experiments).

Cost metrics. We track (i) *forward passes for gradients* (m_c per step during curriculum, m_{train} per step after balance), (ii) *forward passes for candidate evaluation* ($m_c \cdot \lceil \text{search_width} / \text{batch_size} \rceil = m_c \cdot 8$ per step with our default settings), and (iii) *wall-clock time* (total optimization time including GPU memory transfers and batched operations). Optional per-step `model.generate()` calls are counted separately and can be disabled via `enable_step_generate=False` to reduce latency.

Black-box Query Cost Efficiency. An advantage of our transfer-based approach over query-based black-box attacks (e.g., PAIR, TAP, or genetic baselines) is the marginal cost of exploitation. Query-based methods typically require thousands of API interactions to optimize a single adversarial example for a specific target. In contrast, our method optimizes the universal string locally on a surrogate model (incurring zero API cost) and applies it to the target API using a **single inference pass**. For a target dataset of size N , query-based methods incur a cost of $O(N \times Q)$ where Q is the query budget (often > 1000), whereas our approach incurs a cost of $O(N)$ (specifically, $1 \times N$ queries). This makes our attack highly scalable and economically viable against commercial APIs like GPT-4o.

Per-method and per-model statistics. Detailed forward-pass counts and wall-clock times per attack method and model are available in our code repository. For the Qwen2.5-Coder-32B on-target identifier substitution run, the total optimization (including curriculum phase) completes in approximately 20 hours on a single H100. We note that universal GCG amortizes the optimization cost across all target functions, making it more efficient than per-instance optimization when attacking large evaluation sets.

C. Supplementary Result

C.1. Site Selection and Functional Role

To investigate the sensitivity of LLM-based detectors to the spatial placement and syntactic role of adversarial strings, we conducted an ablation study on three models: Qwen2.5-Coder-32B, Llama3.1-8B, and CodeAstra. We focused on two primary dimensions: (i) the **position** of comment-carrier insertions (Leading, Middle, or Trailing) and (ii) the **functional role** of the adversarial pattern in macros (Name vs. Body).

Positional Sensitivity. Table 9 compares the ASR_{cond} for different comment-carrier insertion sites. We observe that *Trailing* comments (placed after the function body) often exhibit high effectiveness, notably for Llama3.1-8B and CodeAstra, where success rates significantly exceed those of the original *Leading* header comments. However, *Middle* placements (interleaved with the logic) often show lower effectiveness across all models. This suggests that the model’s contextual focus on interleaved logic may partially mitigate the influence of semantics-preserving perturbations compared to injections at the function boundaries.

Functional Role Sensitivity. We further analyzed whether the specific role of a string-as part of a macro identifier (*Name*) versus a definition value (*Body*)-affects evasion success. Our results show that *Macro Name* attacks are considerably more potent across all targets. For example, CodeAstra’s resistance increases from 1.13% under Name-based attacks to 69.22% when the pattern is moved to the Body. This indicates that current detectors are particularly susceptible to adversarial signals when they are presented as active code identifiers rather than passive data.

Table 9. Ablation results for different injection sites and functional roles. ASR_{cond} is reported as the fraction of originally correctly detected vulnerable functions (TP_{clean}) that were flipped to BENIGN.

Model	Family	Variant	Flipped / TP_{clean}	ASR_{cond} (%)
Qwen2.5-Coder-32B	Comment	Head (Original)	1026 / 1121	91.53
		Middle	778 / 1121	69.40
		Trailing	952 / 1121	84.92
	Macro	Name (Original)	962 / 1121	85.81
		Body	621 / 1121	55.40
	Llama3.1-8B	Comment	Head (Original)	652 / 1552
Middle			355 / 1552	22.87
Trailing			1163 / 1552	74.94
Macro		Name (Original)	1016 / 1552	65.46
		Body	595 / 1552	38.34
CodeAstra		Comment	Head (Original)	2178 / 3454
	Middle		1565 / 3454	45.31
	Trailing		2941 / 3454	85.15
	Macro	Name (Original)	3415 / 3454	98.87
		Body	1063 / 3454	30.78

D. Extended Sanitization Analysis

Table 10 details prediction drift when applying sanitization (stripping comments and preprocessor directives) to clean, unperturbed vulnerable functions. We measure $\Delta TP = TP_{sanitized} - TP_{original}$, the change in true positive count.

Table 10. Sanitization-induced prediction drift. Stripping benign comments and preprocessor directives from clean code increases vulnerability detection, indicating that non-executable tokens act as lexical distractors.

Model	Original TP	Sanitized TP	ΔTP (%)
Qwen2.5-Coder-32B	1,121	1,179	+58 (+5.17%)
Llama3.1-8B	1,552	1,685	+133 (+8.57%)
CodeAstra	3,454	3,457	+3 (+0.09%)

As shown in Table 10, the detection boundary is highly unstable. For Llama3.1-8B, simply removing developer comments (which have no effect on program execution) causes the model to “discover” 133 previously missed vulnerabilities—an 8.6% increase. This suggests that the model’s clean accuracy is partly contingent on specific lexical distributions rather than robust semantic understanding. Qwen2.5-Coder-32B shows similar behavior (+5.2%), while CodeAstra exhibits minimal drift (+0.09%), suggesting different sensitivities to non-executable context across architectures.

This instability has two implications. First, it confirms that models use syntactically irrelevant tokens as decision features, violating semantic invariance. Second, it undermines sanitization as a defense: while it eliminates carrier surfaces, it simultaneously alters the model’s decision boundary in unpredictable ways, potentially introducing new false negatives or positives on benign code variations.

D.1. Code Length Effect: Additional Results

We measure length using whitespace-delimited token count, i.e., $\text{len}(\text{code.split}())$, and compute correlations with $\text{num_successful_methods} \in \{0, 1, 2, 3, 4, 5\}$ (the number of carriers that flip a clean true positive) on the subset with complete outcomes across all five carriers.

Interpretation. Across models, correlations are often negative but small in magnitude (Table 11), suggesting that longer functions tend to admit fewer successful carriers, with substantial variation by model. One plausible explanation is a dilution effect: as more semantic evidence is present in longer contexts, the marginal influence of a fixed, localized carrier (e.g., a

Table 11. Correlation between code length and joint attack success. Pearson r and Spearman ρ are computed between whitespace token length and `num_successful_methods`.

Model	Pearson r	Spearman ρ
GPT-4o	-0.122	-0.163
GPT-5-mini	-0.172	-0.208
Qwen2.5-Coder-32B	-0.074	-0.069
CodeAstra	-0.068	+0.025
Llama3.1-8B	-0.024	-0.061

header comment or macro name) may diminish. The binned curves in Figure 5 further indicate that the relationship is not purely linear.

Ceiling and variance effects. For Qwen2.5-Coder-32B (and to a lesser extent Llama3.1-8B), the length & robustness association is modest. The joint outcome `num_successful_methods` is skewed toward higher counts when multiple carriers succeed on many samples, which partially attenuates correlation-based summaries. Figure 5 visualizes these partial ceiling effects directly.

Carrier-specific heterogeneity. Length sensitivity is not uniform across carriers. At the carrier level, for Llama3.1-8B, macro-name carriers exhibit a clearer negative trend (Pearson $r \approx -0.163$; Spearman $\rho \approx -0.228$ for whitespace length vs. macro success), while other carriers show weaker dependencies. This pattern is suggestive of carrier-specific coupling, e.g., identifier-like roles may be more susceptible to dilution in longer contexts, but we leave controlled tests (e.g., fixing insertion position and matching structural complexity) to future work.

D.2. Temperature Robustness

Motivation. To verify that attack effectiveness is not an artifact of decoding stochasticity, we repeat the evaluation under two decoding temperatures, $T=0$ (deterministic) and $T=0.7$.

Protocol. For each target model and attack method, we run the full evaluation pipeline at both temperatures under the same prompts and parsing protocol. For stochastic decoding ($T=0.7$), we report mean \pm std over $K=3$ runs.

Results. Table 12 shows that increasing decoding stochasticity does not qualitatively change susceptibility: the union success rate changes only slightly, and per-method success rates remain close across temperatures.

Table 12. Temperature robustness details for GPT-4o. The first row reports overall union success (ASR_{cond}); subsequent rows report per-method $ASR_{\text{cond}}(A; M)$. For $T=0.7$, values are mean \pm std across $K=3$ runs.

Attack Method	$T=0.0$	$T=0.7$ (mean \pm std)
ASR (union)	87.00%	85.19% \pm 0.65%
<code>gcg_var</code>	31.09%	27.85% \pm 0.68%
<code>comment</code>	65.48%	66.06% \pm 0.99%
<code>macro</code>	42.35%	40.62% \pm 0.92%
<code>ifdef</code>	71.61%	74.17% \pm 0.64%

E. Prompt templates

We used the following prompt template (implemented in code as `'get_prompt_template()'`):

```
Strictly analyze code for specific vulnerable variables.
If the label is benign, use empty string for variable.
Output JSON only:
{"label": "VULNERABLE" or "BENIGN", "variable": "<variable_name>"}
```

Do not output explanations. Stop after closing brace.

```
Code:
{func}
```

JSON:

F. Attack Carrier Templates

To ensure full reproducibility, we provide the exact code templates used for each carrier family, corresponding to the implementation logic in our evaluation pipeline. In the templates below, [TRIGGER] denotes the GCG-optimized adversarial string (referred to as {optim_str} in the codebase), and [ORIGINAL_CODE] denotes the victim function text.

F.1. Comment Carrier

We inject a Doxygen-style multi-line comment block immediately preceding the function definition. The adversarial string is embedded within the @commit_hash metadata field, acting as a "distractor" in the non-executable header.

```
/**
 * @brief Function implementation
 * @commit_hash [TRIGGER]
 * @status verified
 */
[ORIGINAL_CODE]
```

F.2. Macro Insertion

We prepend a macro definition before the function. The adversarial string is embedded into the **macro identifier** itself (e.g., SAFE_FUNC_...). This tests the model's sensitivity to token sequences in the global scope that resemble function prototypes but are technically preprocessor directives.

```
#define SAFE_FUNC_[TRIGGER] benign_function()

[ORIGINAL_CODE]
```

F.3. Dead-Branch Insertion

Unlike the preprocessor carriers, this payload is injected **inside** the function body. We locate the final closing brace (}) of the function and insert a strictly dead branch (guarded by if(0)) immediately before it. The adversarial string is encapsulated within a benign string literal statement inside the block.

```
// ... inside the function body ...
// [Insertion Point: before the final return/brace]
if (0) {
    "benign_[TRIGGER]";
}
```

F.4. #ifdef Insertion

We wrap a benign log statement containing the adversarial string within an #ifdef DEBUG_MODE block. This payload is prepended to the function context, simulating a global or static debug configuration common in C/C++ projects. We verified that none of the 5,000 functions in our dataset define or reference common debug macros DEBUG_MODE, eliminating potential risk within our evaluation scope.

```
#ifdef DEBUG_MODE
    benign_log("[TRIGGER]");
#endif

[ORIGINAL_CODE]
```

Semantics-Preserving Evasion of LLM Vulnerability Detectors

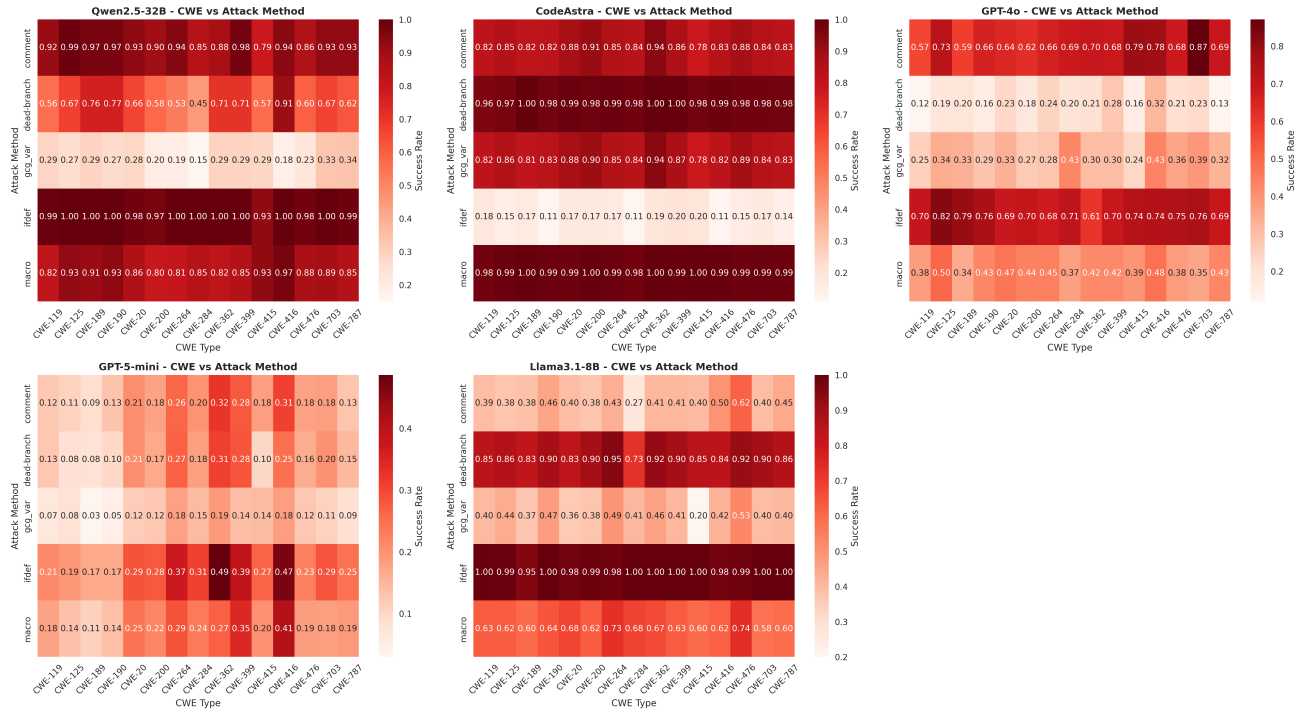


Figure 4. CWE \times attack method success heatmaps across models. Each cell gives the per-method conditional attack success rate $ASR_{cond}(A; M)$ for a given CWE type and attack method. This visualization highlights strong method & CWE interactions and model-specific attack profiles (e.g., CodeAstra’s distinct behavior relative to other models).

E.5. Identifier Substitution

For the identifier substitution attack (not template-based but replacement-based), we identify the target variable v (via the model’s "variable" attribution or frequency analysis) and apply a global string replacement:

```
code.replace(v, [TRIGGER])
```

We strictly validate that [TRIGGER] is a valid C identifier and does not shadow existing symbols in the local or global scope.

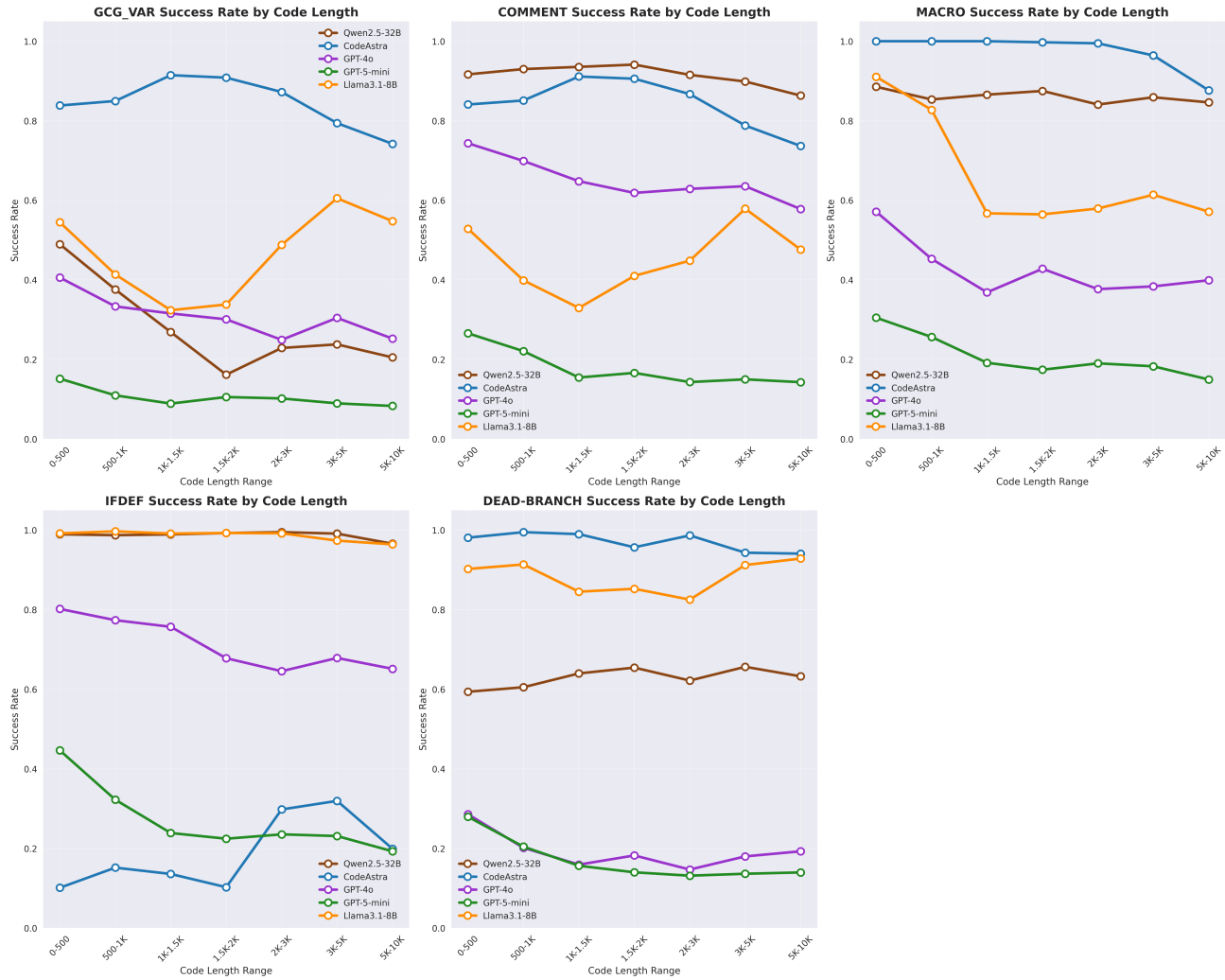


Figure 5. Attack success rate versus code length (binned). Curves show per-carrier success rates across length ranges, complementing Table 11 by revealing non-linear trends and saturation regimes.